RSC Advances

ROYAL SOCIETY OF CHEMISTRY

www.rsc.org/advances

Insights into the effects of γ-irradiation on the microstructure, thermal stability and irradiation-derived degradation components of microcrystalline cellulose (MCC)

Yun Liu [a] *, Jingping Chen [b #], Xiaofeng Wu [c #], Keqin Wang [c] *, Xiaojun Su[d #], Liang Chen [c], Hua Zhou [a], Xingyao Xiong[d, e]

[a] Beijing Key Laboratory of Bioprocessing, College of Life Science and Technology, Beijing University of Chemical Technology, Beijing 100029, China;

[b] Biotechnology Research Center, Hunan Academy of agricultural sciences, Changsha 410125, China;

[c] Hunan Institute of Nuclear Agricultural Science and Space Breeding, Hunan Collaborative Utilization of Botanial Funcational Ingredients, Hunan Academy of agricultural sciences, Changsha 410125, China;

[d] Hunan Provincial Key Laboratory of Crop Germplasm Innovation and Utilization, Hunan Collaborative Innovation for Utilization of Botanical Functional Ingredients, Hunan Collaborative Utilization of Botanial Funcational Ingredients, Hunan Agricultural University, Changsha 410128,China;

[e] The Institute of Vegetables and Flowers Chinese Academy of Agricultural Sciences, Beijing 100081,China

---

# Equal contributor

* Corresponding author: Yun Liu and Keqin Wang

Tel: +86 - 0731-84692317; Fax: +86 -073184691562; Email: liuyunprivate@sina.com or wkq6412@163.com

Abstract

It has been demonstrated that radiation pretreatment can cause a significant breakdown of cellulose stubborn structure, which will increase the accessibility of cellulose and is benefit for enhancing the enzyme hydrolysis in bio-fuel process. In this work, microcrystalline cellulose (MCC) as a model substrate was comprehensively investigated the impacts of irradiated dose on the microstructure, thermal stability and irradiated-degradation components of cellulose under ^{60}Co γ-irradiation circumstances (0 kGy-1400 kGy). FT-IR, EPR and NMR analyses show that irradiation destroys the glycosidic bond and hydrogen bond inter- and intra-molecular of cellulose resulting in the generation of reductive carbonyl group and free radicals. SEM, XRD and GPC analyses confirm that irradiation can damage the crystalline microstructure and morphology surface of MCC, leading to reducing its degree of polymerization from 183045 kDa to 4413 kDa. TGA and DGA curves indicate that activated energy (Ea) and thermal stability of treated MCC decrease with the increasing of irradiation dose. Ion chromatography (IC) analysis demonstrates that there exist fermentation sugars, such as glucose (10.73 mg g^{-1}), xylose (1.58 mg g^{-1}), arabionose (0.46 mg g^{-1}), fructose (4.31 mg g^{-1}), and cellobiose (1.90 mg g^{-1}) as well as low contents of glucuronic acid (0.35 mg g^{-1}) and galacturonic acid (1.46 mg g^{-1}) in the irradiation-derivated degradation components. Therefore, the findings in this work suggest that γ-irradiation processing is an environment-friendly, promising and effective approach to treat lignocellulose biomass.

Keywords: Microcrystalline cellulose (MCC); γ-Irradiation; Microstructure; Thermal stability; Irradiation-derivated degradation components

1. Introduction

Increasing efforts have been made to exploit alternative bioenergy sources from renewable biomasses due to the depletion of fossil fuels and the serious problems of global warming [1]. Lignocellulosic biomass, the most abundant renewable resource all over the world, is a promising feedstock because of non-competition with food and it comprises large amount of cellulose which is considerably converted to ethanol via hydrolysis and fermentation [2, 3]. However, cellulose possesses the crystalline structure and inaccessible morphology hindering the enzymatic conversion from cellulose to fermentation sugars. To improve the accessibility of cellulose, myriads of cellulose pretreatment methods have been intensively developed, such as mechanical ball milling [4], steam explosion [5], dilute acid/alkali [6], supercritical fluids [7], ionic liquids [8-11], ultrasound and radiation pretreatments [12-14]. Among these pretreatment processing, the potential efficient method, therefore, is required to enhance the susceptibility of cellulose by modifying cellulose structure and to minimize the consequent formation of toxic derivatives by degrading cellulose.

Radiation processing like ultrasound [12], electron beam [13], proton beam [15], microwave [16], ionizing irradiation [17, 18] and ^{60}Co γ-irradiation [14, 19], was efficiency to degrade cellulose in biofuels production from biomass. Radiation was successfully applied in lignocellulose pretreatment because it showed the abilities of predominant degradation or depolymerization of cellulose in biomasses, such as bagasse cane, rice straw, wheat straw, and corn stalk [14, 19, 20]. In comparison with other pretreatment methods, radiation uses an applied electromagnetic field to disrupt the microcrystal structure of cellulose in a solid status involving mild temperature, short reaction time and minimal even few undesirable inhibitors [19]. Thus, radiation is highly effective, friendly and energy saving pretreatment processing for lignocellulose ethanol production [19, 20]. However, insights into the degradation mechanism is not systematically available about the effect of γ-irradiation pretreatment on

cellulose under irradiation circumstances, such as the microstructural and morphologic changes, thermalgravimetry and irradiation-derivated degradation components of cellulose before and after treatment.

In this work, ^{60}Co γ-ray irradiation was employed to degrade microcrystalline cellulose (MCC) in solid status under different irradiation doses from 0 kGy to 1400 kGy. The degree of polymerization (DP) was measured by viscosity method to evaluate the extent of scission. Scanning electron microscopy (SEM) was employed to visualize the morphology modification of MCC before and after γ-irradiation treatment. The crystalline index (CrI) of treated MCC was calculated through X-ray diffraction (XRD) spectrum to evaluate the cellulose crystalline type variance. The structural and inter- (intra) molecular bonds changes of treated MCC was analyzed by Fourier transform infrared (FT-IR), electron paramagnetic resonance (EPR), and Nuclear Magnetic Resonance (NMR). The thermal stability properties of MCC were addressed by thermogravimetry analysis (TGA) and differential thermogravimetry (DTG) to calculate activated energy (Ea) in function of irradiation dose. Furthermore, the types and contents of the soluble degradation components of irradiated MCC were measured by ion chromatography (IC). The primary objectives of this work are to elucidate the degradation mechanism of irradiated cellulose, and assess the feasibility and accessibility of γ-ray irradiation as a potential pretreatment method of cellulose for bio-fuel processing.

2. Materials and methods

2.1 Materials

Avicel PH-101 MCC (pharmaceuticals grade, CAS 9004-34-6, particle size 50 μm) was purchased from Sigma-Aldrich Co. in China (Shanghai, China). Nine standards of glucose, fructose, xylose, arabinose, galactose, mannose, cellobiose, galacturonic acid, and glucuronic acid were also bought from Sigma-Aldrich Co. in China (Shanghai, China). Other chemicals

used in this work were analytical reagents and purchased in Beijing locate markets, China.

2.2 MCC irradiation pretreatment

MCC irradiation pretreatment was according to the processing in our previous work [19]. Specifically, all irradiation treatment experiments were performed using a ^{60}Co γ-ray irradiation device at 1.85×10^{16} Bq in the Hunan Irradiation Center (Changsha, China). Approx. 5.0 g dried MCC in a 10 mL sealed glass bottle was set in the device and irradiated at room temperature under ^{60}Co γ-ray irradiation source with the intensity of 9.99×10^{15} Bq and the dose rate of 2.0 kGy h^{-1}. The specific level of ^{60}Co γ-ray irradiation dose was selected as 100 kGy, 200 kGy, 400 kGy, 600 kGy, 800 kGy, 1000 kGy, 1200 kGy and 1400 KGy. The untreated MCC (0 kGy) was as the control sample. After treatment, MCC was homogeneously mixed and employed for the following experimental analyses of morphology, microstructure and irradiated degradation components.

2.3 Scanning electron microscopy (SEM)

At first, MCC sample was homogeneously distributed in deionized water by ultrasonic with a power of 300 W (KQ-300E ultrasonic apparatus, Kunshan, China) for 10 min. After then, a drop of MCC dispersion was applied to single monocrystal silicon gold sheet and dried in vacuum. The morphologies of untreated and treated MCC were imaged by a JSM-6380LV SEM (Japan Electron Optics Laboratory Co., Ltd, Japan) at the working electronic voltage of 10 kV.

2.4 X-ray diffraction analysis (XRD)

XRD measurements were performed to observe the crystalline type change of irradiated MCC against untreated sample at a Rigaku D/max 2500 diffractometer (Rigaku Corporation, Japan) under the following conditions: Cu/Ka wavelength = 0.154 nm, voltage 40 kV, current 250 mA, scanning speed rate 8° min^{-1}, scanning step 0.02° and scanning scale (2θ) 10-40°. Crystalline index (CrI) was calculated from the data of XRD spectrum according to the

method [16] using the intensity of (200) peak (I_{200}, 2θ=22.4º) and the lowest intensity (I_{AM}, 2θ=18º) between the (200) peak (I_{200}, 2θ=22.4º) and (101) peak (I_{101}, 2θ=15.8º) by Eq. (1):

$$\text{CrI (\%)} = \frac{(I_{200} - I_{AM})}{I_{200}} \times 100 \quad (1)$$

where: I_{200} is intensity of (200) peak (at about 2θ=22.4º); I_{AM} is the lowest intensity of the peak at about 2θ=18º.

2.5 Fourier transforms infrared analysis (FT-IR)

KBr pellets of MCC samples were prepared by mixing (1.0-2.0) mg of untreated and treated MCC powder with 200 mg KBr (spectroscopic grade) in a vibratory mixer for 30 s. The pellets of 13 mm diameter were obtained for FT-IR analysis in a standard device under a pressure of 75 kN cm^{-2}. FT-IR spectra were recorded with a Nicolet 670 FT-IR spectrometer (Nicolet NicPlan IR microscope, USA) and using a liquids nitrogen-cooled mercury-caldmium-tellurium (MCT) detector in the regions of 400-4000 cm^{-1}. The running conditions were: resolutions 2 cm^{-1}, scan 64 times, scanning speed 20 kHz.

2.6 Electron paramagnetic resonance (EPR)

EPR spectrum was performed to examine free radicals of cellulose after irradiation and recorded in a JES FA-200 cw-EPR spectrometer (JEOL, Japan) at room temperature. A magnetic field modulation of 4 G and microwave power of 10 mW was used for all experiments to avoid resonance line saturation. EPR intensity data were recalculated per 1 g MCC. The EPR conditions were: microwave frequency 9.06 GHz, microwave power 1 mW, center field 324 mT, initial field 299 mT, sweep width 50 mT, modulation amplitude 0.35 mT, modulation frequency 100 kHz, sweep time 60 s, room temperature. In general, the reproducibility of the EPR measurement for five independent was within 5%.

2.7 Solid state ^{1}H and ^{13}C Nuclear Magnetic Resonance (^{1}H and ^{13}C NMR)

In order to observe the variance of hydrogen bonds intra- and inter-molecular of treated MCC, the cross-polarization/magic angle spinning (CP/MAS) solid state ^{1}H and ^{13}C NMR

were performed at an Avance III 600 NMR spectrometer (Bruker, Switzerland). ^{1}H NMR conditions were: resonance frequency 600.1 MHz, π/2 pulse length 2.57 μs, and delay time 5 s. The conditions of ^{13}C NMR were as follows: resonance frequency 150.9 MHz, CP contact time 2 ms, delay time 5 s. The probe size of CP/MAS was 4 mm and the rotation speed of the rotor was 8 kHz. A number of 300-3175 scans were required to obtain a good signal-to-noise ratio. 4000 accumulations were used for the ^{1}H-^{13}C CP/MAS measurement. Tetramethyl silane (TMS) was used as the reference to determine the chemical shifts of structures.

2.8 Measurement of degree of polymerization (DP)

The average DP of untreated and treated MCC was determined by viscosity measurement in the literature [14]. MCC sample was dissolved in saturated cupriethylenediamine solution. The viscosity of the solution was measured by an Ubbelohde viscometer (Shanghai, China) with capillary (inner diameter 0.6 mm) at 25 °C. The intrinsic viscosity, [η_r], was calculated according to the Martin Eq.(2), and the viscometric DP was calculated according to Immergut formula Eq. (3):

$$\eta_t = \frac{t_i - t_0}{t_0} \tag{2}$$

$$DP = \frac{2000 \times \eta_T}{W \times (1 + 0.29 \times \eta_t)} \tag{3}$$

Where: t_0 and t_i was the consuming time when cupriethylenediamine solution ran through the capillary with and without MCC. W was the weight ratio of MCC in cupriethylenediamine solution.

2.9 Distribution of molecular weight (MW) by gel permeation chromatography (GPC)

To further test the degree of MCC irradiated-dagradation, GPC was carrried out to measure the MW distribution of untreated and treated MCC. The GPC system consisted of an isocratic pump, auto-sampler with thermostat (Agilent 1260 series, Santa Clara, USA), a set of Agilent PLgel MIXED-C (Agilent 1260 GPC，USA) separation columns, and Agilent / HP 1316A

column oven (Agilent 1260 series, Santa Clara, USA). N, N-dimethylacetamide DMAc/LiCl (0.5%, m/V), filtered through 0.45 μm filter, was used as the eluant. The 0.05% MCC in DMAc/LiCl (0.5% m/V) was injected automatically, chromatographed on four serial GPC columns, and monitored by refractive index (RI) detector. MW distribution was calculated by Addon software programs (Agilent Co., USA) based on the refractive index increment of MCC samples. The GPC conditions were: flow rate 1 mL min^{-1}, column Agilent PLgel MIXED-C (7.5 mm × 300 mm, 5 μm), detector RI, injection volume 50 μL, run time 15 min, and temperature 50 °C. The MW deviations of replicate data were within 10%.

2.10 Thermal stability properties measured by thermogravimetry (TG) and differential thermogravimetry (DTG)

The thermodynamic properties of the irradiated MCC samples were assessed using TG and DTG on TGA Q50 thermogravimetric analyzer (Waters Co., USA) under a N_2 atmosphere. About 10 mg of irradiated MCC for each measurement were heated in a platinum crucible from 30 to 900 °C at a heating rate of 20 °C min^{-1}. All measurements were performed under a nitrogen atmosphere at the gas flow rate of 40 mL min^{-1}.

2.11 γ-Irradiated degradation components determination by ion chromatography (IC)

The water soluble fractions of irradiated MCC were determined at room temperature by ICS-3000 ion chromatography (IC) with a refractive index (RI) detector (Dionex, USA) and a CarboPac PA20 column (150 × 3 (i.d) mm, Bio-Rad Labs, USA). NaOH/NaOAc mixture solution was used as mobile phase with the flow rate of 0.5 mL min^{-1}. Other parameters of IC analyses were: Injection volume 25 μL; column temperature 30 °C; gradient eluantion programs at the specific time: NaOH 7 mmol L^{-1} at 0-15min, NaOH 7-100 mmol L^{-1} at 15-20 min, NaOH 100 mmol L^{-1} and NaOAc 100 mmol L^{-1} at 30-40 min, NaOH 200 mmol L^{-1} at 40.1-42.1 min, NaOH 7 mmol L^{-1} at 42.2-46 min. The eluant rate of mobile phase was set at

0.5 mL min^{-1}. Each standard concentration of glucose, fructose, xylose, arabinose, galactose, mannose, cellubiose, galacturonic acid, and glucuronic acid was fixed at 1.0 mg mL^{-1}.

3. Results and discussion

3.1 Effects of γ-irradiation pretreatment on the microstructure of MCC

SEM analysis. The impacts of γ-irradiation on the surface morphology of treated MCC were visualized by SEM and are shown in Fig. 1. Holes in melton form can be clearly observed on the surface of the treated MCC with more than 400 kGy, whereas the surface of untreated MCC is comparatively smooth. The damage degree of MCC morphology surface is much greater with increasing of absorbed dose from 100 kGy to 1400 kGy. This irradiation-derived damage of MCC morphology will significantly influence the substantial structural and thermal stability properties of MCC. This observation agrees well with that by Sun and co-workers [14], who demonstrated that cracks and trenches were clearly observed on the surface of the MCC samples irradiated with 500 kGy. In our previous works, it was also apparent to observe that the morphology surface of cellulose was damaged when γ-irradiation was subjected to pretreating ligninocellulose biomasses, such as baggase cane, corn stalk, rice straw, and *Phragmites communis* trim [19, 20]. Therefore, γ-irradiation pretreatment can easily disrupt the microstructure of MCC to disorder the cellulose molecular arrangement, which enhances the susceptibility of cellulose and achieves almost complete enzymatic digestibility for bioethanol production [21].

XRD analysis. Figure 2 shows the XRD spectra of MCC irradiated with different absorbed doses from 100 kGy to 1400 kGy. The characteristic peaks at about 15.8°, 22.4°, and 34° lattices and the crystalline parameters of the untreated and treated MCC were obtained by deconvoluting the spectra with Jade 5.0 XRD software. The data were summarized in Table 1. In comparison with the untreated MCC, it is obviously found that CrI values have an apparent change as a function of the absorbed doses, and decrease gradually from 75% to 58% leading

to the formation of amorphous cellulose when the absorbed dose increases up to 1200 kGy. This observation implies that the crystalline structure of the irradiated MCC may be remarkably damaged, which is ascribed to fragment of hydrogen bond in the MCC molecular. Sun and co-workers [14], however, found that the dimensions of the crystal lattice did not change evidently (Crl only decreased from 68% to 61%) during the absorbed dose below 500 kGy. Furthermore, some researchers demonstrated that crystalline transformation of cellulose showed significant effects on enzymatic digestibility and enzyme loading for following saccharification [4, 21].

Distribution of molecular weight (Mw) and DP Analysis. It has been demonstrated that cellulose polymer would de-polymerize and reduce molecular weight in presence of γ-irradiation [14, 19, 20]. Table 2 summarizes the effect of γ-irradiation on the distribution of molecular weight and DP variances of MCC irradiated with different adsorbed doses from 100 kGy to 1400 kGy. It can be seen from the last line in Table 2 that the DP of MCC is reduced from 183045 to 4413 under the irradiation of 1200 kGy, and the decrease of DP with further increasing of the absorbed dose gradually slows down when the irradiation dose is ranging from 400 kGy to 1200 KGy. Simultaneously, Mw, Mn, Mz, Mv and Mp distributions decrease steeply when the irradiation dose is up to 1200 kGy. It may be ascribed to the fact that MCC surface has suffered from an irradiation- mediated oxidation degradation that eases further attacks on the molecule [14]. However, In Table 2, it seems that there is sometimes increasing in Mz, Mz+1 and Mp at irradiation doses of either 1000 or 1200 kGy. The reasonable explanation might be attributed to measurement errors. But the overall tendency of molecular weight distribution is decreasing with increasing of irradiation dose in our work. From the values of polydispersity indexes (1.7-1.5) in the second line from the bottom in Table 2, it can be found that the irradiation makes the cellulose molecules tend to homogenization and small particle size, which may be attributed to irradiation-mediated

oxidation degradation leading to chain scission [22]. All these obseversions are consistent with previous studies of SEM and XRD in this work.

FT-IR analysis. The FT-IR spectra of the MCC irradiated with different absorbed doses are depicted in Fig. 3. It is known that irradiated cellulose by high absorbed dose in the presence of oxygen will lead to the formation of carbonyl and carboxyl groups due to oxidative degradation [14, 22]. Compared with the untreated MCC (0 kGy), it is obviously observed in Fig. 3 that the characteristic peak of around 1732 cm^{-1} ascribed to the carbonyl groups (C=O stretching vibration) is formed at 200 kGy, and the intensity of this peak at 1732 cm^{-1} increases gradually with the increasing absorbed dose up to 1200 kGy. Furthermore, the band at around 3300 cm^{-1} attributed to the vibration of hydrogen bonded OH-groups shifts to lower wave number firstly (at 200 kGy) and then to higher wave number when the absorbed dose exceeds 400 kGy. Such shifts indicate that γ-irradiation interrupts the intra-molecular and inter-molecular hydrogen bonds in cellulose [23, 24]. At lower absorbed dose (e.g. at 200 kGy), γ--irradiation mainly destroys the original intra-molecular hydrogen bonds and the peak at around 3300 cm^{-1} shifts to lower wave number (3200 cm^{-1}). Further increasing irradiation dose up to 1200 kGy, the new formation of carbonyl groups becomes stronger, which strengthens the hydrogen bond of C=O…H-O resulting in red shift to high wave number (3400 cm^{-1}) at higher absorbed doses [23, 24]. The absorbance at 2899 cm^{-1} used as a reference is ascribed to the C-H stretching vibration. The findings suggest that the process of MCC degradation is accompanied with the formation of carbonyl groups containing compounds [14]. It can also be found from Fig. 3 that the vibration wave numbers at 1164 cm^{-1}, 1112 cm^{-1} and 1058 cm^{-1} all shift to lower wave number and the intensities of these bands become stronger with the increase of irradiated doses. Such shifts suggest that γ-irradiation probably interrupt the intermolecular C-O-C bond of cellulose due to irradiation-mediated oxidative degradation [25]. According to the reports in reference [23],

the assignments of all these peak wave numbers are shown in Table 3.

^{1}H and ^{1}C CP/MAS NMR In order to evaluate the bonds cleavage in cellulose backbone, solid-state NMR spectroscopy was employed to assess the functional group changes of MCC before and after irradiation treatment, which can provide not only chemical shift information but also chemical environment and ultra-structural details. These information is not easily accessible by other non-destructive high-resolution spectral techniques [26]. It is noteworthy that there are three noticeable changes in the character of the ^{1}H NMR spectra (Fig. 4). Firstly, the total ^{1}H intensity increases significantly when irradiated doses enhance gradually up to 1200 kGy. Secondly, the ^{1}H line shape enlarge apparently with increasing irradiated dose from 200 kGy to 1200 kGy. Thirdly, the high peak of H nuclei at about 5 ppm of MCC shift when irradiated dose increased up to 1200 kGy. These shifts of ^{1}H NMR spectra of treated MCC are ascribed to a substantial increase of hydrogen nuclei during irradiation-induced degradation. From the ^{13}C CP/MAS NMR spectra (Fig. 4), carbon chemical shifts and the intensity of carbon peaks for the C_1, C_4 and C_6 ring positions in the cellulose backbone are changed in the presence of irradiation. These slight changes of carbon chemical shifts of irradiated MCC probably result in its microstructure from crystalline type to amorphous formation, which agree well with the findings of XRD analysis in this work. From solid state ^{1}H and ^{13}C-NMR spectra, it can be reasonably drawn a conclusion that treated MCC undergoes an oxidative degradation and provide positive charge (H^+) during this degradation processing when MCC is subjected to high irradiated doses environment.

EPR investigation As seen in Fig. 5, there exist significant differences in the EPR signals of untreated and irradiated MCC. Obviously, no EPR signal is observed for MCC untreated, whilst the EPR signals of irradiated MCC significantly represent weak triplet with relative intensity. It is reasonably speculated that free radicals are formed during irradiation processing of MCC and a large increase in radical concentration occurs at high irradiation dose. The

triplet spectrum consists of the central line, which is buried by the natural intense singlet, and two weak characteristic satellite lines separate ca. 2 mT left and right to it. It is probably attributed to the formation of weak charge-transfer complexes when MCC is subjected to high adsorbed dose of γ-irradiation circumstances [14]. The formation of free radicals was directly on the cellulose backbone by cleaving the C_2-C_3 bond and oxidation of cellulosic chain ends containing hemiacetal linkages. This observation agrees well with the result in NMR analysis in our work. Paukszta reported that other pretreatment methods such as thermal and mechanical treatments of lignocellulose also might result in free radicals generation [27]. Undoubtedly, EPR method can be used for distinguishing irradiated from non-irradiated samples of certain cellulose-containing foods stocks from the view of free radicals formation [28].

3.2 Effects of absorbed dose on thermal stability of cellulose

To address the thermal properties of treated MCC, thermal gravimetric analysis (TGA) and differential thermal analysis (DTA) curves of MCC irradiated with different absorbed doses are shown in Fig. 6.

As seen in Fig. 6, the TGA curves of the irradiated MCC appear to be divided into three weight loss phases. At the first stage, the initial weight loss mainly happens in the region between 50 °C and 150 °C due to the dehydration. This change at the first stage was also called as physical change [29]. The endothermic peak appears on the DTA curves at about 150 °C. Moisture content (%) in MCC between 50 °C and 150 °C increases with the increasing absorbed dose. From the previous findings of XRD, FT-IR and NMR, irradiation can disrupt the crystalline structure of MCC, and generate some amount of hydrophilic groups such as carbonyl group, carboxyl group, and free hydroxyl group, which result in a higher hygroscopicity of irradiated MCC at higher irradiated doses. At the second stage, the major weight loss occurs between 200 °C and 500 °C. The absorbed dose increasing from 0 to 1200

kGy, the onset temperature (T_i) of the depolymerization and decomposition of MCC decreases from 300 °C to 150 °C, respectively. Also, the terminative temperature (T_f) gradually increases from 390 °C to 550 °C when the absorbed doses increased from 200 kGy to 1200 kGy. At the point about 310 °C, exothermal peaks appear in this stage on the DTA curve. At the second stage, the DTA peaks become wider and move to the lower temperature regions, which indicates that the maximum temperature (Tp) of highest weight loss reduces with increase of irradiated dose. Figure 7 shows the dependence of absorbed dose on the peak temperature Tp at which the rate of degradation reaches the maximum value. It can be noticed that Tp decreases from 390 °C to 305 °C with the increase of absorbed dose from 0 kGy to 1200 kGy, which is coincident with the effect of absorbed dose on DP. The reduction of DP is the main cause resulting in degeneration of thermal stability of treated MCC. On the other hand, the slight decreasing in crystallinity as observed in XRD also decreases the thermal stability of irradiated MCC. DTA peaks become wider because of the presence of a large number of low molecular weight fragments, random distributed cleavages, and breakdowns of C-O-C units in cellulose chains [14]. The radiation degradation not only decreases the DP of MCC but also leads to the wider distribution of molecular weight [14]. This result also reflects the randomicity of the radiation degradation [30]. At the third stage, the weight loss is not very evident. The exothermal peaks change into relatively smooth ones, which indicate that the rates of weight loss slow down. About 10% residue solid is left at 1200 kGy. Taken together, no obvious difference of thermal stability is observed for MCC irradiated with different absorbed doses from 200 kGy to 1200 kGy.

To further elucidate the effect of absorbed doses on thermogravimetry of MCC, the thermogravimetric kinetics was estimated to calculate activated energy (Ea) using Coats-Redfern equation as follows Eqs. (4) and (5):

$$\frac{d_\alpha}{d_t} = A \times \exp\left(-\frac{E_a}{RT}\right) \times (1-\alpha)^n \quad (4)$$

$$\alpha = (m - m_T)/(m - m_2) \quad (5)$$

where: m is the mass weight of MCC, g; m_T is the mass weight of MCC at temperature of T °C, g; m_2 is residue mass weight of MCC, g; t is the treated time, s; R is the molar gas constant, J/K. mol; T is the temperature, °C; E_a is the activated engery, kJ/mol.

When the rising rate of temperature is considered as β, K min^{-1}, Eq. (4) could be transferred to Eq. (6):

$$\int_0^\alpha \frac{d_\alpha}{(1-\alpha)^n} = \frac{A}{\beta}\int_0^T \exp\left(-\frac{E_a}{RT}\right) dT \quad (6)$$

Consuming $\frac{E_a}{RT} = u$, Eq. (7) can be obtained as follows:

$$du = \frac{E_a \times dT}{RT^2}, \text{ and then } dT = \frac{RT^2}{E_a} \times du \quad (7)$$

Combining Eqs. (6) and (7), and further simplifying, Then, Eq. (8) could be obtained as follows:

$$\int_0^\alpha \frac{d_\alpha}{(1-\alpha)^n} = \frac{A}{\beta}\int_0^T e^{-u}\left(-\frac{E_a}{RT}\right) du = \frac{AE_a}{\beta R} u^{1-2} e^{-u} \sum_{n=0}^{\infty} \frac{(-1)\times 2^n}{u^{n+1}}$$

$$= -\frac{AR}{\beta E_a}\left(1 - \frac{2RT}{E_a}\right) e^{-\frac{E_a}{RT}}$$

$$\ln\left[\frac{d_a}{T^2}\right] = \ln\left[\frac{AR}{\beta E_a}\left(1 - \frac{2RT}{E_a}\right)\right] - \frac{E}{RT} \quad (8)$$

In this study, $\frac{E}{RT} >> 1$, so $\ln\left[\frac{AR}{\beta E_a}\left(1 - \frac{2RT}{E_a}\right)\right]$ becomes almost a constant number.

Therefore, the relationship between $\ln\left[\frac{d_a}{T^2}\right]$ and $\frac{1}{T}$ is a linear curve. From the slope and

intercept, *Ea* can be obtained.

Linear fit is performed on the thermogravimetric curves using Coats-Redfern method in presence of different irradiated doses and the results are shown in Fig. 8. It is apparently seen that the *Ea* of irradiated MCC decreases with the increasing of irradiated dose. The reasonable explanation is the fact that the crystalline structure of irradiated MCC is destroyed leading to decrease its thermal stability. The findings are consistent with the results of FT-IR, SEM, XRD and NMR in previous experiments of this work.

3.3 Effects of absorbed dose on irradiation-derived degradation components of cellulose

As noted above, γ-irradiation pretreatment could disrupt the cellulose crystalline structure, and yield both soluble and insoluble fractions. Therefore, the soluble fractions of irradiation-mediated degradation components comprise some water-soluble sugars, including C_5 and C_6 monomers, cellobiose, as well as the toxic by-products inhibitors, such as galacturonic and glucuronic acids. The water-soluble sugars and glucuronic and galacturonic acids of irradiated MCC were measured by ion chromatography (IC), and the results are summarized in Table 4.

Generally seen in Table 4, the water-soluble sugars of the irradiated MCC at 1200 kGy are composed of relatively high concentration of glucose (10.73±0.42 mg g^{-1}), fructose (4.31±0.14 mg g^{-1}), cellobiose (1.90±0.03 mg g^{-1}) and xylose (1.58±0.09 mg g^{-1}). Very little amount of arabinose (0.46±0.01 mg g^{-1}) at the dose of 1200 kGy is observed, but mannose is almost not available in this work. It is interesting to notice that the contents of water-soluble sugars (glucose, fructose, xylose and cellobiose) of irradiated degradation components of MCC increase with increasing of irradiation doses from 100-1400 kGy. Meanwhile, very low content of glucuronic acid (0.35±0.00 mg g^{-1}) is detected among the irradiation-mediated degradation components. In our previous work, we compared the effect of steam explosion and irradiation pretreatments on the inhibitors among degradation components of rice straw

materials. Interestingly, no glucuronide acid was detected in irradiation pretreated rice straw, while glucuronide acid with the content from 8.5 mg/g to 9.2 mg/g was obtained in steam explosion pretreated sample [19]. On the other hand, low content of galacturonic acid (1.46±0.06 mg g-1) at 1400kGy are detected in the MCC irradiated degradation components. It was reported that glucuronic and galacturonic acids are toxic compounds inhibitors to the yeast fermentation from biomass hydrolysis for bioethanol production [31, 32].

4. Conclusions

High γ-Irradiation pretreatment can evidently disrupt the crystalline microstructure of MCC, resulting in reducing DP and thermal stability. Irradiation influences the inter- and intra-molecular hydrogen bond of MCC and generates carbonyl groups contained compounds. Apart from C_5 and C_6 monosugars and cellobiose, irradiation-mediated degradation components consist of low content of inhibitors, such as glucuronic and galacturonic acids. Efficiency eliminating the negative effects of these inhibitors on yeast fermentation is ongoing in our lab. In conclusions, irradiation positive effects on cellulose will benefit the conversion of lignocellulose to ethanol using enzyme hydrolysis and fermentation.

Abbreviations

MCC: Microcrystalline cellulose. DP: Degree of polymerization. SEM: Scanning electron microscopy. FT-IR: Fourier transforms infrared spectrometry. EPR: Electron paramagnetic resonance. NMR: Nuclear Magnetic Resonance. CP/MAS: Cross-polarization/magic angle spinning. XRD: X-ray diffraction. TGA: Thermogravimetry analysis. DTG: Differential thermogravimetry. IC: Ion chromatography. Ea: Activated energy. MW: Molecular weight. GPC: Gel permeation chromatography.

Acknowledgements

This work was funded by the National Natural Science Foundation of China (NSFC, 31070709), the Program of the Co-construction with Beijing Municipal Commission of

Education of China (506209), "863" Program of High Technology Research and Development of China (2012AA101804), Special Fund for Agro-scientific Research in the Public Interest (201503135), and Innovation Team Project of Hunan Province Academy of Agricultural Sciences (2014TD03).

References

[1] Yue D, You F, Snyder SW. Biomass-to-bioenergy and biofuel supply chain optimization: Overview, key issues and challenges. Comput Chem Eng 2014; 66: 36-56.

[2] Miller SA. Sustainable polymers: Opportunities for the next decade. ACS Macro Lett 2013; 2: 550-4.

[3] Anbarasan P, Baer ZC, Sreekumar S, Gross E, Binder JB, Blanch HW, et al. Integration of chemical catalysis with extractive fermentation to produce fuels. Nature 2012; 491: 235-9.

[4] Peng H, Li H, Luo H, Xu J. A novel combined pretreatment of ball milling and microwave irradiation for enhancing enzymatic hydrolysis of microcrystalline cellulose. Bioresource Technol 2013; 130, 81-7.

[5] Li G, Chen H. Synergistic mechanism of steam explosion combined with fungal treatment by *Phellinus baumii* for the pretreatment of corn stalk. Biomass Bioenerg 2014; 67: 1-7.

[6] Singh J, Suhag M, Dhaka A. Augmented digestion of lignocellulose by steam explosion, acid and alkaline pretreatmentmethods: A review. Carbohyd Polym 2015; 117: 624-31.

[7] Gu T, Held M A, Faik A. Supercritical CO_2 and ionic liquids for the pretreatment of lignocellulosic biomass in bioethanol production. Environ Technol 2013; 34: 1735-49.

[8] Hsu W-H, Lee Y-Y, Peng W-H, Wu KC-W. Cellulosic conversion in ionic liquids (ILs): Effects of H_2O/cellulose molar ratios, temperatures, times, and different ILs on the production of monosaccharides and 5-hydroxymethylfurfural (HMF). Catal Today 2011; 174: 65-9.

[9] Su Y, Brown HM, Li G, Zhou X, Amonette JE, Fulton JL, Camaioni DM, Zhang ZC. Accelerated cellulose depolymerization catalyzed by paired metal chlorides in ionic liquid

solvent. Appl Catal A-Gen, 2011; 391: 436-42.

[10] Long J, Guo B, Teng J, Yu Y, Wang L, Li X. SO3H-functionalized ionic liquid: Efficient catalyst for bagasse liquefaction. Bioresour Technol 2011; 102: 10114-23.

[11] Kuo I-Jg, Suzuki N, Yamauchi Ye and Wu KC-W. Cellulose-to-HMF conversion using crystalline mesoporous titania and zirconia nanocatalysts in ionic liquid systems. RSC Adv, 2013; 3: 2028-34.

[12] Karimi M, Jenkins B, Stroeve P. Ultrasound irradiation in the production of ethanol from biomass. Renew Sust Energ Rev 2014; 40: 400-21.

[13] Lee BM, Lee JY, Kang PH, Hong SK, Jeun JP. Improved Pretreatment Process Using an Electron Beam for Optimization of Glucose Yield with High Selectivity. Appl Biochem Biotech 2014; 174: 1548-57.

[14] Sun J, Xu L, Ge M, Zhai M. Radiation Degradation of Microcrystalline Cellulose in Solid Status. J Appl Polym Sci 2013; 127: 1630-6.

[15] Kim SB, Kim JS, Lee JH, Kang SW, Park C, Kim SW. Pretreatment of Rice Straw by Proton Beam Irradiation for Efficient Enzyme Digestibility. Appl Biochem Biotech 2011; 164: 1183-91.

[16] Moretti MMD, Bocchini-Martins DA, Nunes CDC, Villena MA, Perrone OM, da Silva R, Boscolo M, Gomes E. Pretreatment of sugarcane bagasse with microwaves irradiation and its effects on the structure and on enzymatic hydrolysis. Appl Energ 2014; 122: 189-95.

[17] Driscoll MS, Stipanovic AJ, Cheng K, Barber VA, Manning M, Smith JL, et al. Ionizing radiation and a wood-based biorefinery. Radiat Phys Chem 2014; 94: 217-20.

[18] Charlesby A. The degradation of cellulose by ionizing radiation. J Polymer Sci 1955; 15: 263-70.

[19] Wang K, Xiong X, Chen J, Chen L, Su X, Liu Y. Comparison of gamma irradiation and steam explosion pretreatment for ethanol production from agricultural residues. Biomass

Bioenerg 2012; 46: 301-8.

[20] Wang K, Xiong X, Chen J, Chen L, Liu Y. Effect of ^{60}Co-γ irradiation on the microcrystalline cellulose structure of *Phragmites communis* trim. Wood Fiber Sci 2011; 43: 225-31.

[21] Horikawa Y, Konakahara N, Imai T, Kentaro A, Kobayashi Y, Sugiyama J. The structural changes in crystalline cellulose and effects on enzymatic digestibility. Polym Degrad Stabil 2013; 98: 2351-6.

[22] Milanovic J, Schiehser S, Milanovic P, Potthast A, Kostic M. Molecular weight distribution and functional group profiles of TEMPO-oxidized lyocell fibers. Carbohyd Polym 2013; 98: 444-50.

[23] Oh SY, Yoo DI, Shin Y, Kim HC, Kim HY, Chung YS, et al. Crystalline structure analysis of cellulose treated with sodium hydroxide and carbon dioxide by means of X-ray diffraction and FTIR spectroscopy. Carbohyd Res 2005; 340: 2376-91.

[24] Schwanninger M, Rodrigues JC, Pereira H, Hinterstoisser B. Effects of short-time vibratory ball milling on the shape of FT-IR spectra of wood and cellulose. Vib Spectrosc 2004; 36: 23-40.

[25] Yang GS, Zhang YP, Wei MY, Shao HL, Hu XC. Influence of γ-ray radiation on the structure and properties of paper grade bamboo pulp. Carbohydr Polym 2010; 81: 114-9.

[26] Foston M. Advances in solid-state NMR of cellulose. Curr Opin Biotech 2014; 27: 176-84

[27] Paukszta D. Mercerisation of Rapeseed Straw Investigated with the Use of WAXS Method. Fibres Text East Eur 2013; 21: 19-23.

[28] Yordanov ND, Gancheva V. A new approach for extension of the identification period of irradiated cellulose-containing foodstocks by EPR spectroscopy. Appl Radiat Isotopes 2000; 52: 195-8.

[29] Bian J, Peng F, Peng X-P, Xu F, Sun R-C, Kennedy JF. Isolation of hemicelluloses from sugarcane bagasse at different temperatures: Structure and properties. Carbohyd Polym 2012; 88: 638-45.

[30] Qua EH, Hornsby PR, Sharma HSS, Lyons G. Preparation and characterisation of cellulose nanofibres. J Mater Sci 2011; 46: 6029-45.

[31] van Maris AJA, Abbott DA, Bellissimi E, van den Brink J, Kuyper M, Luttik MAH, et al. Alcoholic fermentation of carbon sources in biomass hydrolysates by *Saccharomyces cerevisiae*: current status. Anton Leeuw Int J G 2006; 90: 391-418.

[32] Tissot C, Grdanovska S, Barkatt A, Silverman J, Al-Sheikhly M. On the mechanisms of the radiation-induced degradation of cellulosic substances. Rad Phy Chem 2013; 84: 185-90.

Figure captions

Figure 1 SEM images of MCC before irradiation (0 kGy) and after irradiation at 200 kGy, 400 kGy, 600 kGy, 800 kGy, 1000 kGy, 1200 kGy and 1400 kGy.

Figure 2 XRD pattern of MCC irradiated with different absorbed doses at 0 kGy, 200 kGy, 400 kGy, 600 kGy, 800 kGy, 1000 kGy and 1200 kGy.

Figure 3 FT-IR spectra of MCC irradiated with different adsorbed doses at 0 kGy, 200 kGy, 400 kGy, 600 kGy, 800 kGy, 1000 kGy and 1200 kGy.

Figure 4 ^{1}H MAS NMR and ^{1}C CP/MAS NMR spectra of MCC irradiated with different doses at 0 kGy, 200 kGy, 400 kGy, 600 kGy, 800 kGy, 1000 kGy and 1200 kGy.

Figure 5 EPR spectra of MCC irradiated with different doses at 0 kGy (g), 200 kGy (f), 400 kGy (e), 600 kGy (d), 800 kGy (c), 1000 kGy (b) and 1200 kGy (a).

Figure 6 T thermogravimetry curves of MCC irradiated with different doses at 0 kGy (g), 200 kGy (f), 400 kGy (e), 600 kGy (d), 800 kGy (c), 1000 kGy (b) and 1200 kGy (a).

Figure 7 The dependence of absorbed doses from 200 kGy to 1200 kGy on the peak temperature Tp

Figure 8 Linear fit curves of the MCC thermogravimetric data using Coats-Redfern method in presence of different irradiated doses at 0 kGy, 200 kGy, 400 kGy, 600 kGy, 800 kGy, 1000 kGy and 1200 kGy.

Fig.1

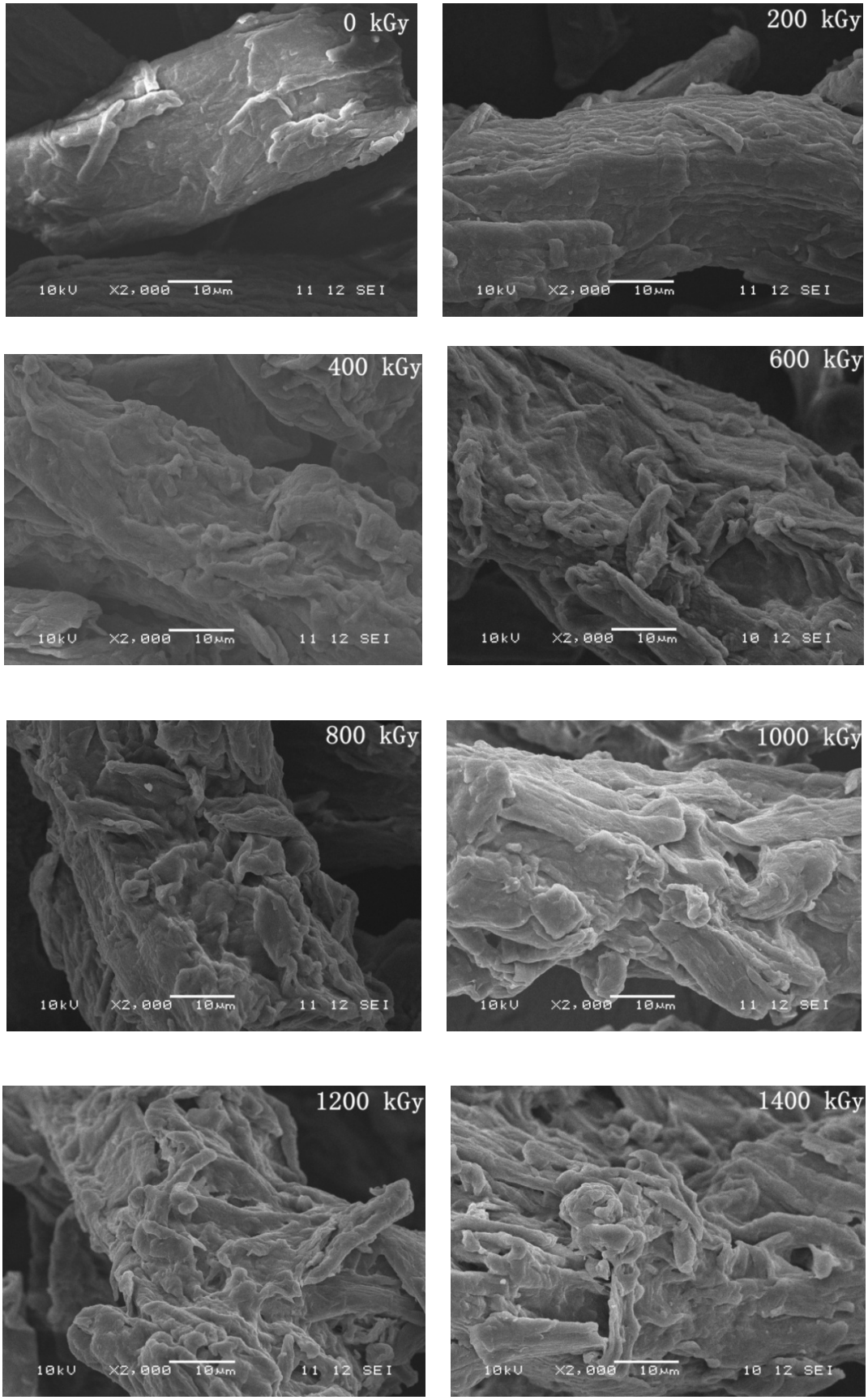

Fig. 2

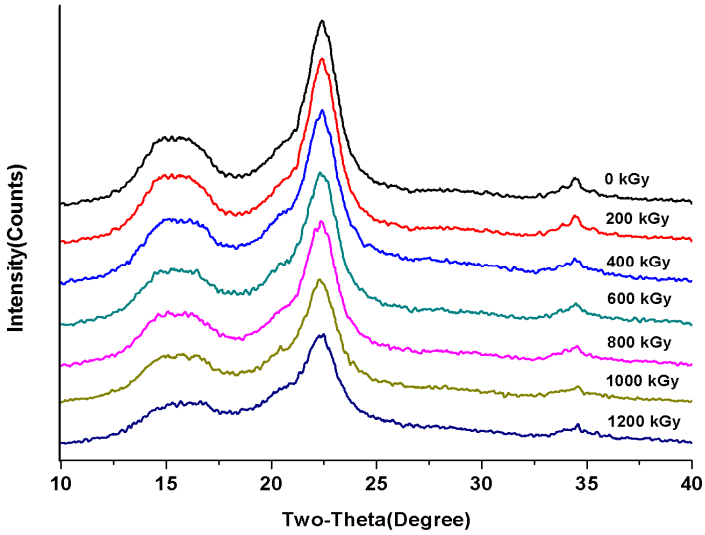

Fig. 3

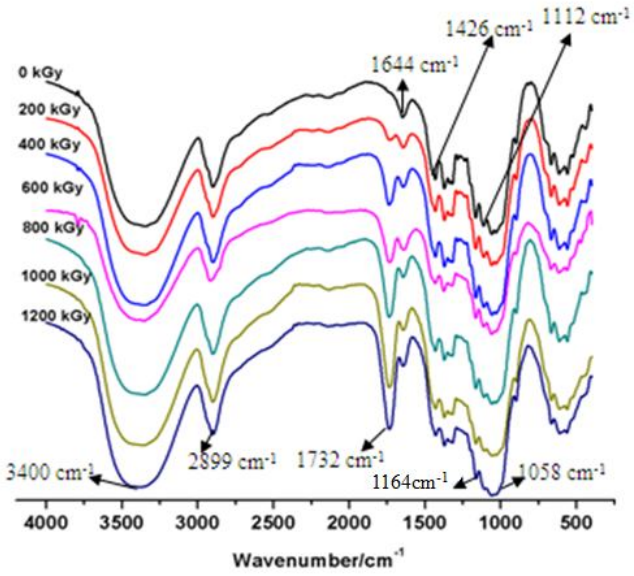

Fig. 4

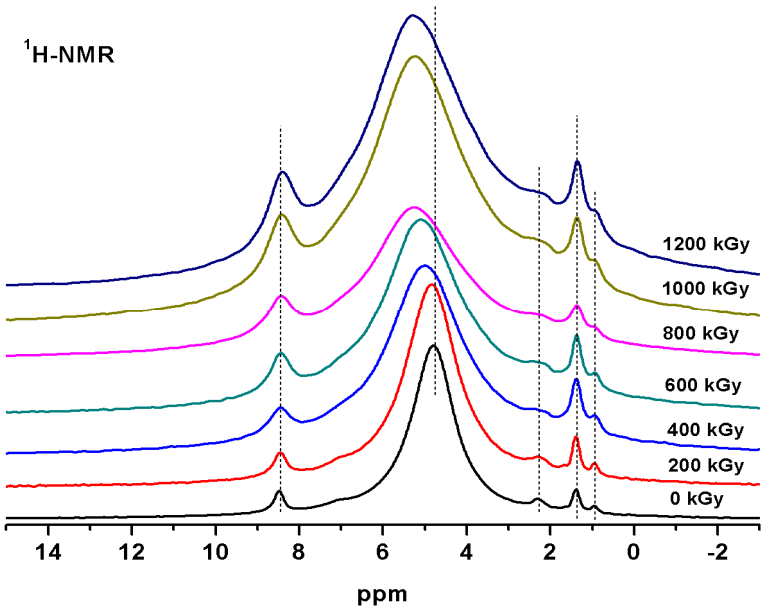

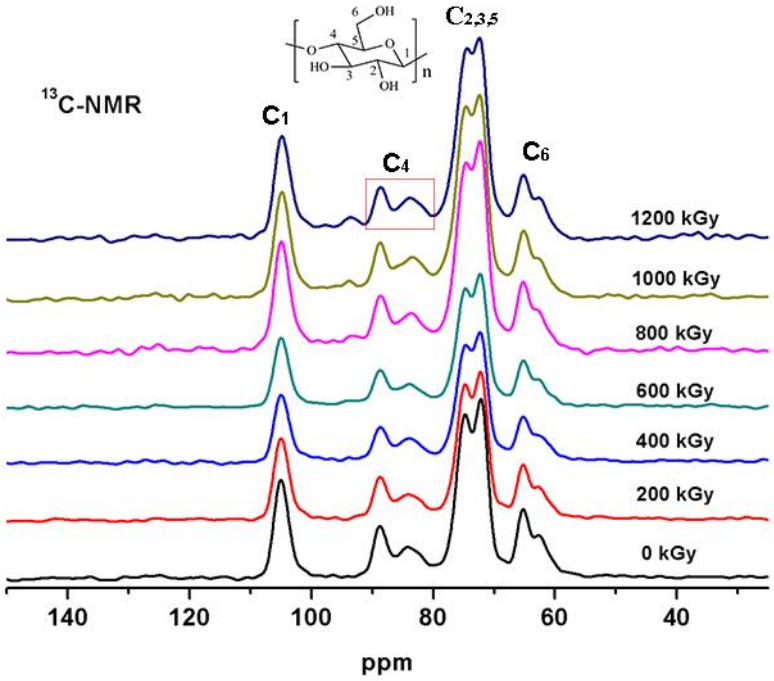

Fig. 5

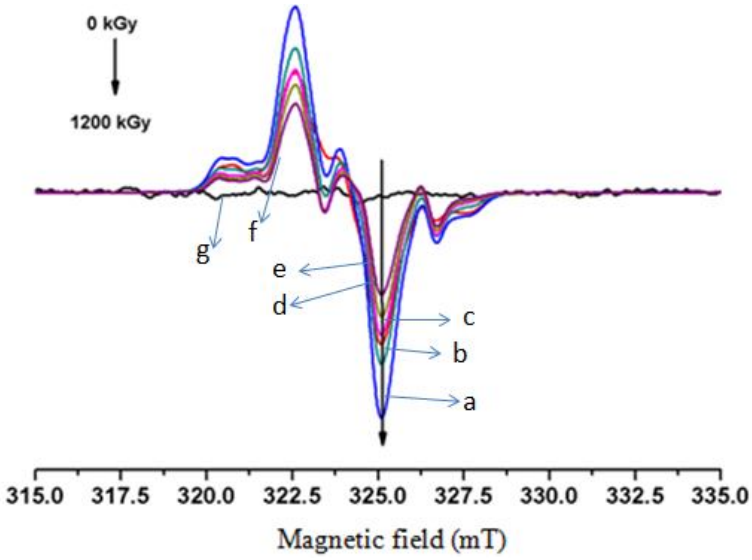

Fig. 6

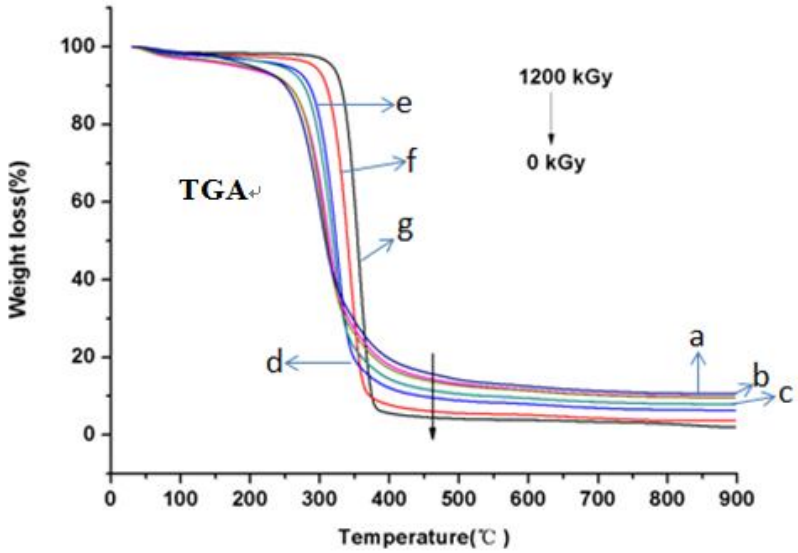

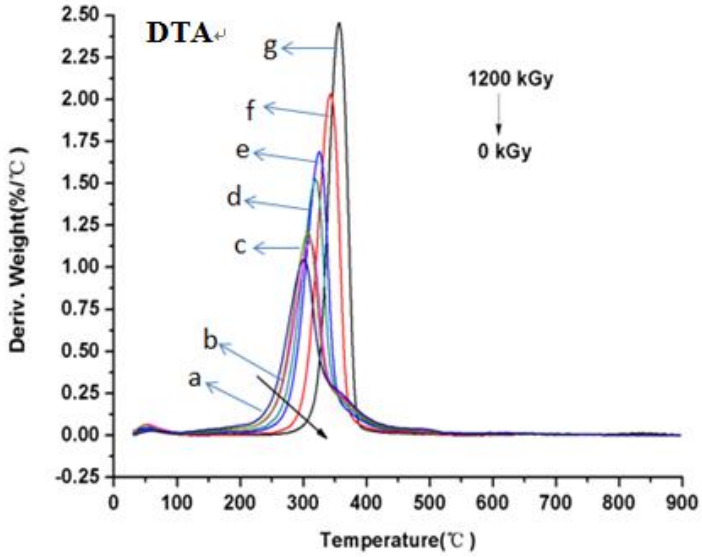

Fig. 7

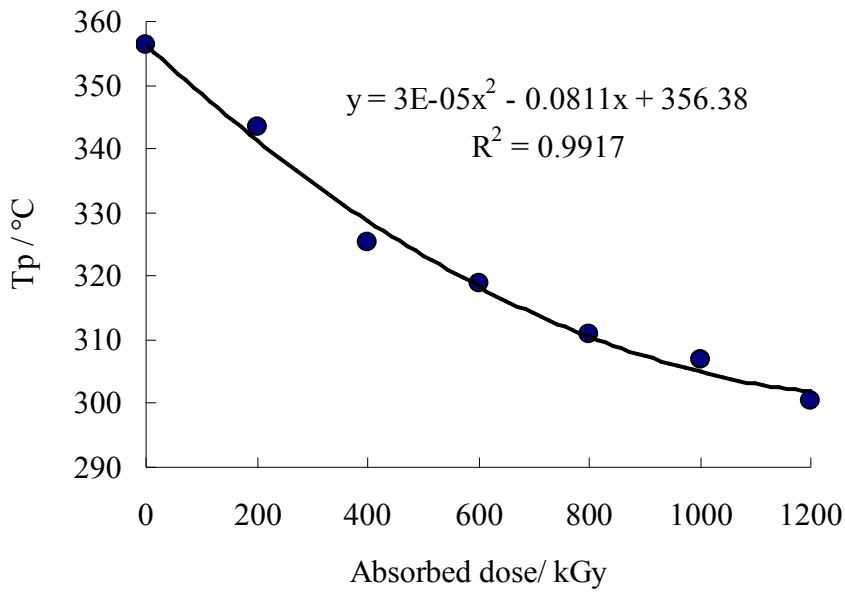

Fig. 8

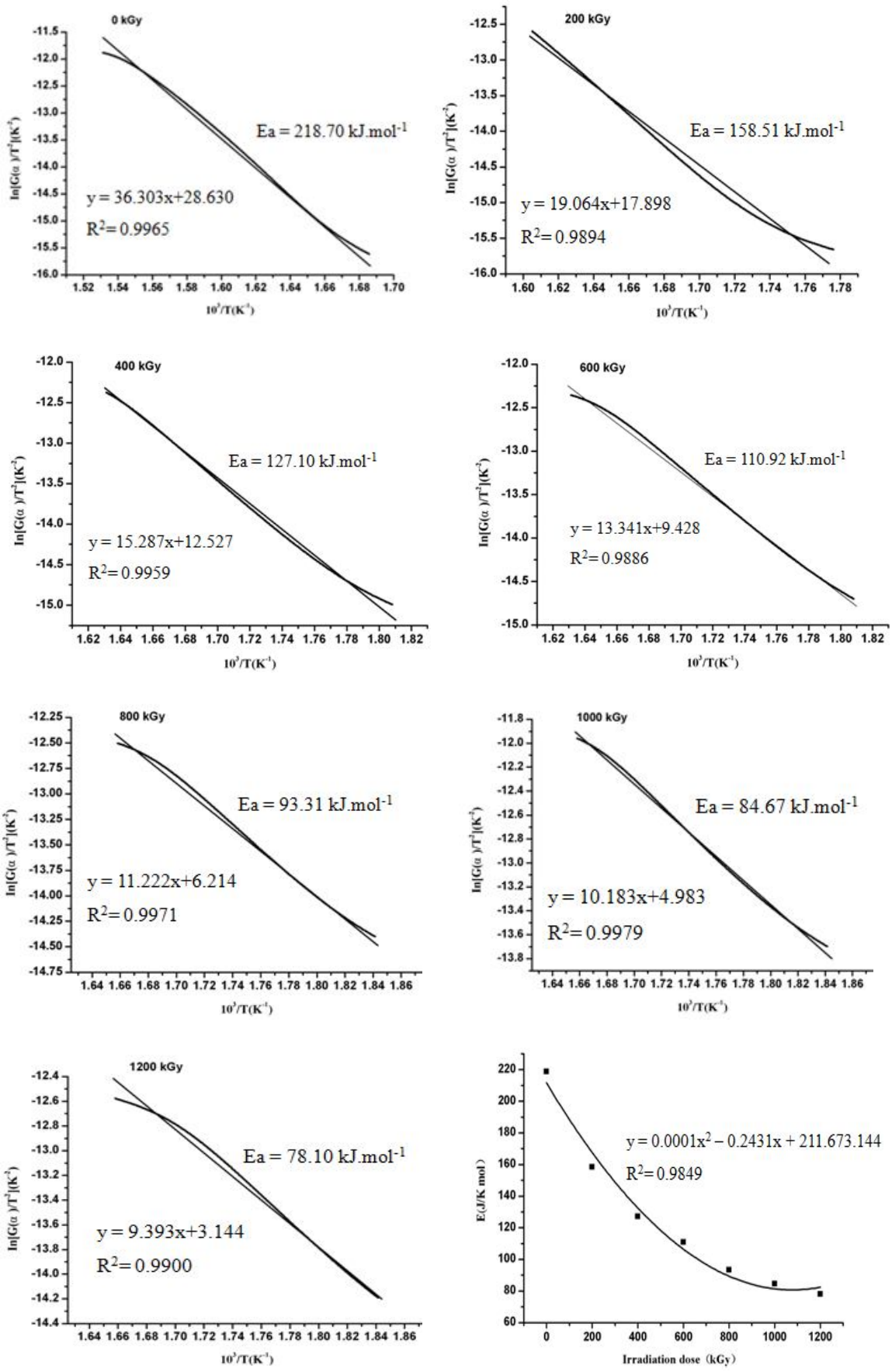

Table 1 Characterization peaks and CrI (%) of MCC irradiated with different absorbed doses

Absorbed doses (kGy)	Location of characterization peaks			CrI (%)
	I_{101} (15.8º)	I_{AM} (18º)	I_{200} (22.4º)	
0	480	273	1115	75.52
200	506	334	1106	69.80
400	428	302	944	68.01
600	377	278	823	66.22
800	368	274	751	63.51
1000	356	297	734	59.54
1200	315	278	667	58.32

Table 2 Effect of adsorbed dose on molecular weight distribution and DP of MCC

Adsorbed doses (kGy)	0	400	600	800	1000	1200
Weight-average Molecular Weight (Mw, Da)	189591	56610	46839	36221	35973	33336
Number-average Molecular Weight (Mn, Da)	65174	32182	28321	23680	24059	22933
Z-average molecular weight (Mz, Da)	2637259	109455	96275	92689	85470	89270
Z+1-average molecular weight (M_{z+1}, Da)	36150445	265055	348634	550648	502651	602031
Viscosity-average molecular weight (Mv, Da)	164682	53093	44080	34143	34060	31562
Peak molecular weight (Mp, Da)	134310	49604	23645	20726	21480	20974
Ratio of Mz/Mw	13.91	1.933	2.055	2.559	2.376	2.678
Ratio of Mz+1/Mw	190.67	4.682	7.443	15.202	13.973	18.06
polydispersity index (ratio of Mw/Mn)	2.909	1.759	1.654	1.53	1.495	1.454
Degree of polymerization (DP)	183045	47495	30700	17340	9137	4413

Table 3 Peak wave numbers of FT-IR bands and their assignments according to the literature

Wave number (cm^{-1})	Band origin (assignment) with comments
3340-3450 cm^{-1}	Valence vibration of bonded OH-groups (intra-molecular) or inter-molecular in cellulose
2898-2899 cm^{-1}	-CH, $-CH_2$ valence vibration in cellulose from C_6
1731-1735 cm^{-1}	C=O valence vibration of acetyl- or COOH-groups
1654-1642 cm^{-1}	H-O-H valence vibration in adsorbed water
1428-1431 cm^{-1}	$-CH_2$ scissoring
1371-1372 cm^{-1}	-CH deformation vibration
1315-1318 cm^{-1}	$-CH_2$ rocking vibration
1161-1164 cm^{-1}	C-O-C asymmetric valence vibration
1111-1119 cm^{-1}	C-O stretching
1057-1058 cm^{-1}	C=O valence vibration
894-898 cm^{-1}	β,1-4 glycosidic bond

Table 4 MCC irradiated degradation components at different absorbed dose

Irradiated dose (kGy)	Glucose (mg g^{-1})	Fructose (mg g^{-1})	Arabionose (mg g^{-1})	Mannose (mg g^{-1})	Xylose (mg g^{-1})	Cellobiose (mg g^{-1})	Glucuronic acid (mg g^{-1})	Galacturonic acid (mg g^{-1})
0	n.a.	n.a.	0.02±0.03	n.a.	n.a.	n.a.	n.a.	0.04±0.03
100	0.08±0.11	0.00±0.00	0.03±0.05	n.a.	0.00±0.00	0.04±0.05	n.a.	0.03±0.04
200	0.42±0.08	0.08±0.11	0.10±0.01	n.a.	0.06±0.01	0.50±0.12	n.a.	0.13±0.04
400	2.26±0.03	0.89±0.00	0.18±0.04	n.a.	0.37±0.01	0.50±0.01	0.02±0.00	0.26±0.05
600	3.14±0.25	0.95±0.23	0.22±0.01	n.a.	0.49±0.04	0.64±0.02	0.05±0.00	0.37±0.03
800	5.15±0.10	2.03±0.12	0.32±0.01	0.14±0.01	0.87±0.01	1.04±0.04	0.20±0.02	0.69±0.10
1000	5.68±0.00	2.65±0.03	0.34±0.03	0.13±0.01	0.95±0.06	1.24±0.01	0.22±0.00	0.80±0.06
1200	6.79±0.01	2.96±0.07	0.41±0.00	n.a.	1.14±0.12	1.40±0.06	0.35±0.02	1.05±0.06
1400	10.73±0.42	4.31±0.14	0.46±0.01	n.a.	1.58±0.09	1.90±0.03	0.35±0.00	1.46±0.06

n.a. means not available

Graphical abstract

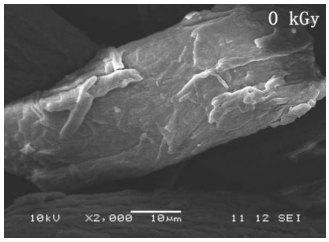

γ -Irradiation pretreatment

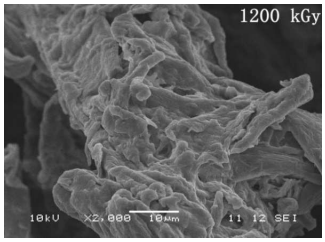

Microcrystalline cellulose(MCC) before pretreatment

Microcrystalline cellulose(MCC) after pretreatment

The microstructure, thermal stability and irradiated-degradation components of microcrystalline cellulose were investigated under ^{60}Co γ-irradiation circumstances (0 kGy-1400 kGy).